A systematic comparison of four pharmacopoeial methods for measuring powder flowability

Weeraya Tharanon ^a , Yiwang Guo ^b , Jomjai Peerapattana ^{a,*} , Changquan Calvin Sun ^{b,*}
^a Division of Pharmaceutical Technology, Faculty of Pharmaceutical Sciences, Khon Kaen University, Khon Kaen 40002, Thailand
^b Pharmaceutical Materials Science and Engineering Laboratory, Department of Pharmaceutics, College of Pharmacy, University of Minnesota, Minneapolis, Minnesota 55455, USA
* C 1'
* Corresponding to:
jomsuj@kku.ac.th (Jomjai Peerapattana)
sunx0053@umn.edu (Changquan Calvin Sun)

1 Abstract

Powder flow is one of the crucial factors affecting several pharmaceutical manufacturing 2 processes. Problems due to insufficient powder flow reduce production process efficiency and 3 cause suboptimum product quality. The U.S. Pharmacopoeia has specified four methods to 4 evaluate the flowability of pharmaceutical powders, including angle of repose (AoR), 5 6 compressibility index (CI) and Hausner ratio (HR), Flow through an orifice, and shear cell. 7 Comparison within and between those methods with 21 powders (covering a wide range of flowability) was performed in this study. Strong correlation was observed between fixed base cone 8 AoR, and fixed height cone AoR ($R^2 = 0.939$). CI and HR values calculated from a tapped density 9 tester (meeting USP standards), manual tapping, and Geopyc® correlated strongly (R²> 0.9). AoR, 10 CI/HR, minimum diameter for flowing through an orifice (d_{min}), and shear cell results generally 11 correlate strongly for materials with flowability worse than Avicel® PH102. Both shear cell and 12 CI/HR methods can reliably distinguish powders exhibiting poor flow. For materials with good 13 flow, the ability to distinguish powders follows the order of AoR \approx CI/HR > shear cell > d_{min} . The 14 systematic comparison of the four common methods provides useful information to guide the 15 16 selection of methods for future powder flow characterization. Given the limitations observed in all four methods, we recommend that multiple techniques should be used, when possible, to more 17 18 holistically characterize the flowability of a wide range of powders.

- 19 **Key words**: powder flow, angle of repose, shear cell, compressibility index, Hausner ratio, flow
- 20 through an orifice

1. Introduction

Powder flow plays an important role in various pharmaceutical manufacturing processes, such as tablet and capsule production. Insufficient powder flow due to inherently poor flowability or suboptimal process design causes problems, such as flow obstruction, segregation, and uneven flow (Buanz, 2021; Schulze, 2021; Staniforth, 2001). Such problems can, in turn, reduce production process efficiency and cause suboptimum product quality. For example, poorly flowing powders can exhibit inconsistent tablet or capsule filling, resulting in poor content uniformity, large weight variation, and variable tablet mechanical strength, disintegration, and drug release performance (Chattoraj et al., 2011; Gaisford and Saunders, 2012; Staniforth, 2001; Sun, 2010; Thalberg et al., 2004). Moreover, industrial production frequently requires powder transportation from one manufacturing plant to another or one operation unit to another within the same manufacturing site. A key requirement towards effectively controlling powder flow behaviors or solving flow-related problems during manufacturing is clear understanding of powder flow properties based on appropriate characterization of powders using established techniques.

The onset of powder flow requires the motion of individual particles within the powder, which is induced by a state of non-equilibrium forces. Depending on the nature of the material and surrounding environment, forces acting on a particle in a powder bed at rest may include gravitational force, adhesion and cohesion force, electrostatic force, magnetic force, water bridges, friction, or forces due to mechanical interlocking (Gaisford and Saunders, 2012; Staniforth, 2001). The interplay among these forces depends on several factors, such as particle size and size distribution, particle shape, environmental conditions (e.g., humidity, temperature, acceleration, and gravitational constant), as well as some other factors, such as the angle of inclination, mass of the powder pile, and applied load (Gaisford and Saunders, 2012; Goh et al., 2018; Schulze, 2021; Staniforth, 2001).

Methods for characterizing powder flow properties can be broadly categorized as static and dynamic (Krantz et al., 2009). A static method is generally performed on a static powder bed, such as angle of repose (AoR), shear cell, tapped and untapped bulk density, critical orifice diameter. A dynamic method characterizes powders in motion under well-defined conditions, including the measurement of hopper flow rate, and flow rate by a recording flow meter (Staniforth, 2001; Taylor and Aulton, 2021). For pharmaceutical powders, the U.S. pharmacopoeia has specified four

methods, i.e., AoR, compressibility index (CI) and Hausner ratio (HR), flow through an orifice, and shear cell, in the monograph <1174> "powder flow" (USP, 2020a). Other useful techniques for flowability evaluation of powders are both dynamic, e.g., fluidization method (Krantz et al., 2009; Leturia et al., 2014; Lüddecke et al., 2021), avalanching method using a rotating drum (such as Aeroflow® device) (Hancock et al., 2004; Lavoie et al., 2002; Taylor et al., 2000; Thalberg et al., 2004), powder rheometry (FT4 powder rheometer) (Bharadwaj et al., 2010; Freeman, 2007) and static, e.g., ball indentation method (Hassanpour et al., 2019; Zafar et al., 2015).

Given the complexity of powder flow, each of these methods focuses only on one or some aspects of the properties of powder flow. Hence, evaluating a powder using different methods simultaneously is highly beneficial to gain a holistic understanding of powder flowability (USP, 2020a). For examples, several excipients were studied using AoR, CI, HR, and shear cell methods in the context of capsule filling (Tan and Newton, 1990). Flowability of powders for inhalation were characterized by HR, AoR, avalanching, and shear tester methods (Thalberg et al., 2004). Effects of particle size and shape on flowability of a few drug formulations were studied using AoR, HR, powder rheometry, shear cell, and avalanching methods (Goh et al., 2018). Flowability of several metal powders were characterized by flow rate, HR, AoR, shear cell, and rheometer (Marchetti and Hulme-Smith, 2021). Effects of particle size, morphology, and density on flowability of microcrystalline cellulose powders were investigated using a shear cell method and CI (Hou and Sun, 2008). However, to our knowledge, there is not yet a report that systematically compared the four methods in the U.S. Pharmacopoeia monograph <1174> using several powders that cover a wide range of flowability (cohesive to excellent flow). Hence, this study was carried out to fill the knowledge gap.

2. Materials and Methods

2.1. Materials

Five grades of microcrystalline cellulose (MCC), including Avicel[®] PH105, PH101, and PH102 (International Flavors & Fragrances, Philadelphia, PA) and Comprecel[®] M101 and M102 (Mingtai Chemical, Taoyuan, Taiwan), milled alpha-lactose monohydrate (Pharmatose[®] 200M; DMV-Fonterra Excipients, Goch, Germany), spray dried lactose (Fast-flo[®]; Foremost Farm

Middleton, WI, USA), spray dried lactose (FlowLac ®100, Meggle GmbH & Co. KG, Wasserburg am Inn, Germany), fluid bed agglomerated lactose (Supertab® 24AN; DFE Pharma, Goch, Germany), native glutinous rice starch (nGRS; General Food Products, Nakhon Ratchasima, Thailand), spray-dried rice starch (Era-tab®; Erawan Pharmaceutical Research and Laboratory, Thailand), mannitol (Pearlitol® 160C; Roquette, Lestrem, France), sodium chloride (NaCl; Macron Fine Chemicals, Center Valley, PA), and co-processed lactose and microcrystalline cellulose (Microcelac®100) and co-processed lactose, microcrystalline cellulose, and maize starch (Combilac®) from Meggle GmbH & Co. KG (Wasserburg am Inn, Germany) were used as received. Spray dried glutinous rice starch (sGRS) and co-processed glutinous rice starch (CP-GRS) prepared in our laboratories by spray-drying were also included in this study. CP-GRS consists of the Thai glutinous rice starch and MCC (Comprecel® M101) and milled α-lactose monohydrate.

2.2. Methods

2.2.1. Preparation of mixtures

Three mixtures between Avicel® PH101 and Avicel® PH102 in ratios of 1:1, 1:2, 2:1 and a mixture of native glutinous rice starch, Comprecel® M101, and milled α -lactose monohydrate in the 3:1:1 ratio (corresponding to the composition of CP-GRS) were prepared using a blender operated at 49 rpm for 10 min (Turbula, Glen Mills, Clifton, NJ). The batch size was 100 g for all mixtures. The inclusion of mixtures in this study was intended to systematically vary powder flow characteristics for testing so that we can better compare different flow testing methods.

2.2.2. Flowability measurement

2.2.2.1. Angle of repose

Angle of repose (AoR) is the angle formed between the slope and the base of the conical heap of a powder. It describes the propensity of particles to roll down a pile under the influence of gravity, which is hindered by interparticle friction and adhesion. A lower AoR is thought to represent better flow property and a powder flowability classification based on AoR has been proposed (Table 1) (USP, 2020a). We have converted the USP flow classification to a simplified scheme, with flow levels from 1 to 7.

Table 1. Flowability classification based on angle of repose (AoR) (USP, 2020a)

Flow property	AoR (°)	Level
Excellent	25–30	1
Good	31–35	2
Fair—aid not needed	36–40	3
Passable—may hang up	41–45	4
Poor—must agitate, vibrate	46–55	5
Very poor	56–65	6
Very, very poor	>66	7

The AoR can be measured by different methods (USP, 2020a). The basic AoR method employs a fixed funnel, where either the pile height is fixed while allowing the cone diameter to vary (known as fixed height cone method or fixed funnel and free standing cone method) or the cone diameter is fixed while allowing the pile height to vary (known as fixed base cone or fixed bed cone) (Buanz, 2021; Kalman, 2021; Montanari et al., 2017; Train, 1958; USP, 2020a). There are some variations of the AoR methods, such as drained AoR (internal flow funnel method), dynamic AoR (revolving cylinder or rotating drum method), hollow cylinder method (lifting cylinder method), tilting box method, and tilting cylinder method (Beakawi Al-Hashemi and Baghabra Al-Amoudi, 2018; Müller et al., 2021; USP, 2020a). The fixed funnel method, using both fixed base and fixed height, was used in this study.

For the fixed height method (Fig. 1a), powder was poured through a glass funnel (Pyrex[®], Corning, Glendale, Arizona) with 100 mm top inner diameter, 8 mm stem inner diameter, and 60° wall angle. Since the method is not specified in the USP, we followed the method described by Train (1958). Here, the funnel was set at a position with the tip 3 cm above a flat paper base. The powder was carefully poured through the funnel while avoiding any disturbance to the funnel. Pouring was stopped when the heap touched the funnel tip. The diameter of the base of the cone was determined with a digital caliper (Digimatic, Mitutoyo Corporation, Kawasaki, Japan). The AoR, α , was calculated using Eq. 1 (USP, 2020a).

 $\operatorname{Tan}(\alpha) = 6 / d$ Eq. 1

where d is the diameter of the base of the cone in cm.

For the fixed base cone method (Fig. 1b), which was modified from the USP method (USP, 2020a), a powder was carefully poured through the funnel onto a flat circular base with a diameter of 7 cm. The funnel height was carefully adjusted to maintain a distance of 2-3 cm between the heap apex and the funnel tip throughout the process. Pouring stopped when the powder fully covered the base (Fig. 1b). A photo of the pile was captured from the side, which was processed to obtain an AoR value from both sides of the heap using an open source image processing software, ImageJ (version 1.53k) (Rasband, 1997). The average of two angles was taken as AoR. All AoR experiments were done in triplicate for each powder.

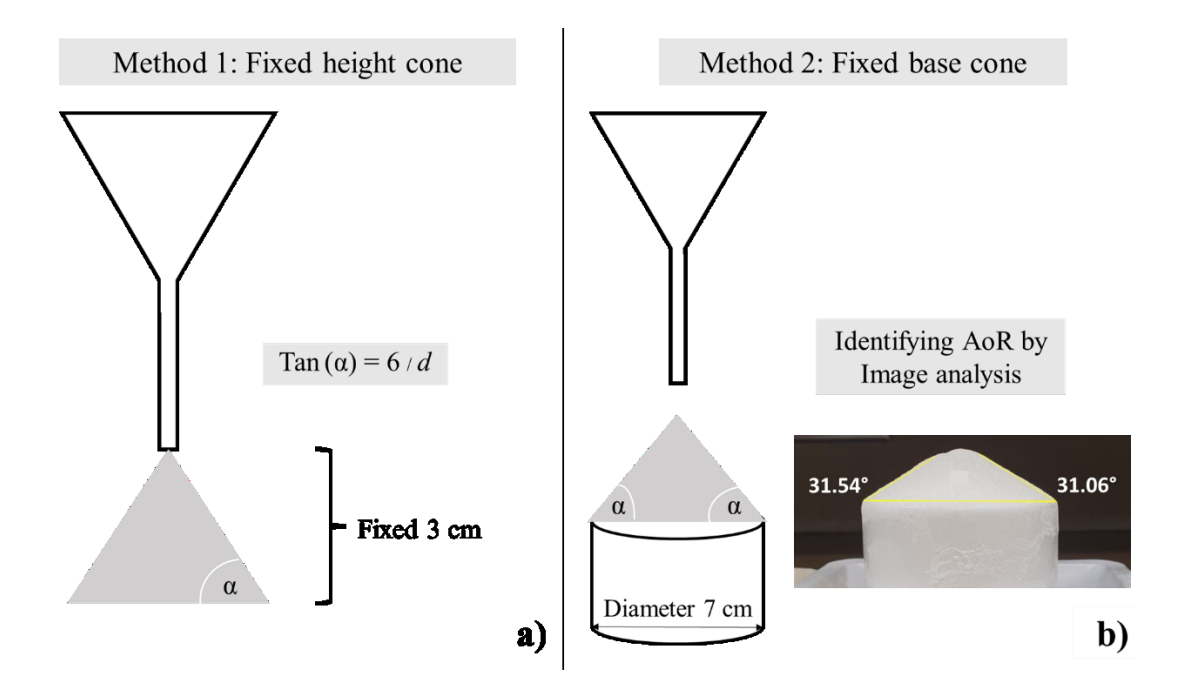


Fig. 1. Experimental setup for measuring AoR: a) fixed height cone b) fixed base cone

2.2.2.2. Compressibility index and Hausner ratio

The compressibility index (CI) and Hausner ratio (HR) were calculated from tapped (V_{tapped}) and untapped bulk powder volumes (V_{untapped}), using Eqs. 2 and 3, respectively (USP, 2020a).

146
$$CI\% = 100 \text{ x } [(V_{\text{untapped}} - V_{\text{tapped}}) / V_{\text{untapped}}]$$
Eq. 2
$$HR = V_{\text{untapped}} / V_{\text{tapped}}$$
Eq. 3

CI and HR can also be calculated from untapped bulk density ($\rho_{untapped}$) and tapped bulk density (ρ_{tapped}) using Eq. 4 and Eq. 5, respectively (USP, 2020a). These CI and HR values are identical to values from volume-based calculations using Eqs. 2 and 3 because powder weight cancels out in the calculation.

152
$$CI\% = 100 \text{ x } [(\rho_{tapped} - \rho_{untapped})/\rho_{tapped}]$$
 Eq. 4

HR = $\rho_{tapped}/\rho_{untapped}$ Eq. 5

The bulk volume of a powder includes the interparticulate volume (void volume between particles), intraparticulate (pore volume inside the solid particles), and solid volume (Buanz, 2021). The untapped bulk density ($\rho_{untapped} = weight/V_{untapped}$) is also known as 'poured' or 'fluff' or 'aerated' bulk density (Gaisford and Saunders, 2012; Harnby and Vandame, 1987; Thalberg et al., 2004). After being tapped or shaken, a powder assumes a more efficient packing arrangement, resulting in a smaller volume (V_{tapped}) and higher density (ρ_{tapped}). The ρ_{tapped} is sometimes also termed 'consolidated density' or 'final density' (Gaisford and Saunders, 2012). For the same material, a finer powder with a lower bulk density usually exhibits both larger CI/HR and poorer flowability because of higher cohesion among particles. On this basis, CI and HR have been used to assess powder flowability, with a greater CI or HR indicates a more cohesive powder and poorer flow (Table 2) (Montanari et al., 2017). Here, we also converted the USP scale to a simpler scale, ranging from 1 to 7.

To determine CI and HR in this work, a powder was passed through a 1 mm mesh-sieve (No. 18) before testing to maintain the maximum porosity of the materials and minimize the compression effect from the filling process (Buanz, 2021). Three techniques were used to determine CI and HR in this study (Fig. 2) and each measurement was done in triplicate.

Table 2. CI and HR general flowability scale (Modified from USP, 2020a)

Compressibility index (%)	Flow Property	Hausner Ratio	Level
≤ 10	Excellent	1.00-1.11	1
11-15	Good	1.12-1.18	2
16-20	Fair	1.19-1.25	3
21-25	Passable	1.26-1.34	4
26-31	Poor	1.35-1.45	5
32-37	Very poor	1.46-1.59	6
> 38	Very, very poor	> 1.60	7

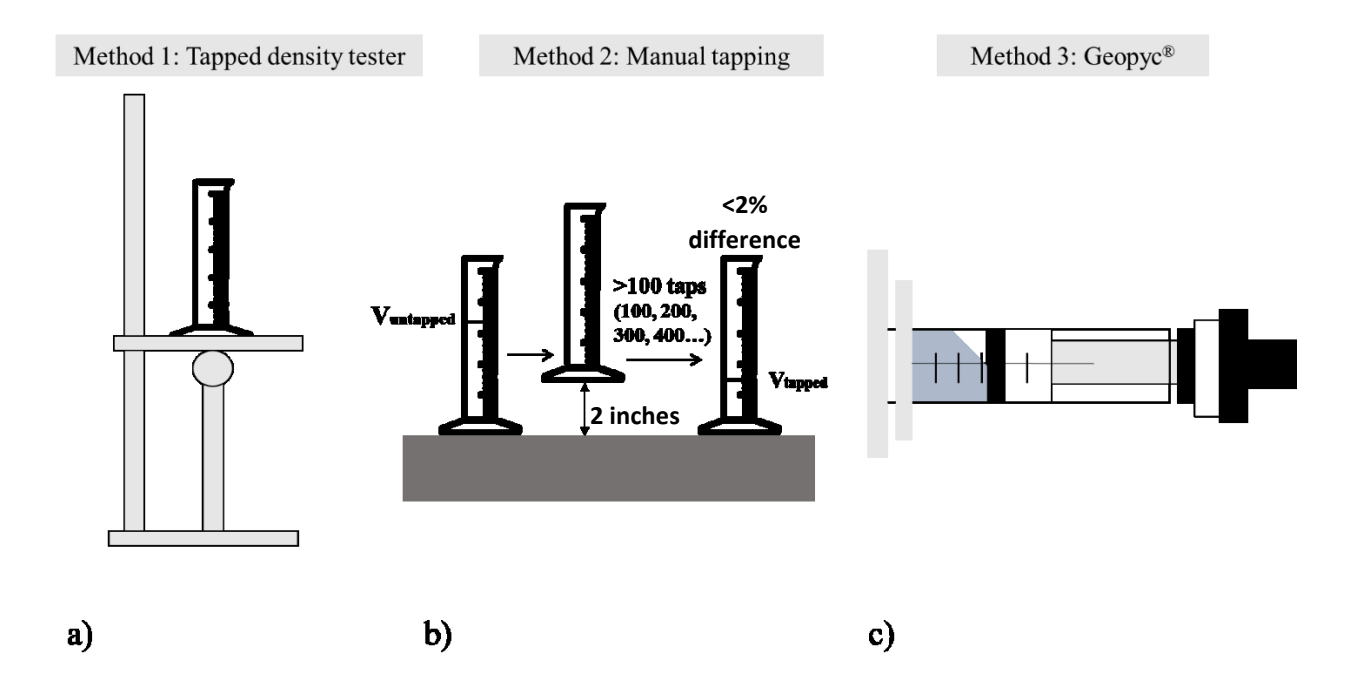


Fig. 2. Experimental methods to measure V_{untapped} , V_{tapped} , ρ_{untapped} , and ρ_{tapped} to derive CI and HR by a) tapped density tester b) manual tapping c) Geopyc[®]

2.2.2.3. Tapped bulk volume and density

Following the method described in USP (Fig. 2a), a powder was slowly added into a tilted 100 mL graduated cylinder until 2/3 of the cylinder was filled. The cylinder was then carefully lifted to the standing position and an initial bulk volume, read to the nearest graduated unit, was taken as $V_{\rm untapped}$, from which $\rho_{\rm untapped}$ can be calculated if powder weight is known. The cylinder was placed on a tapped density tester (TD1, SOTAX, Aesch, Basel-Landschaft, Switzerland) and tapped for 10, 500, and 1250 times. The corresponding volume after each set of tapping was read to the nearest graduated unit. The final $V_{\rm tapped}$ was determined when the volume changed between two readings was less than 1 mL (USP, 2020c). In this study, the difference between V_{500} and V_{1250} was less than 1 mL in all powders. Therefore, V_{1250} was taken as $V_{\rm tapped}$ for calculating CI (Eq. 2) and HR (Eq. 3).

In a variation of the USP tapped density method (Fig. 2b), ten grams of powder was weighed and slowly added into a tilted 50 mL graduated cylinder. The cylinder was carefully lifted to the upright standing position and an initial bulk volume ($V_{\rm untapped}$) was read. The cylinder was vertically lifted to a well-controlled height of around 2 inches and allowed to fall onto a padded bench top. The volume changes after every 100 times were calculated and the final reading was taken as the tapped volume ($V_{\rm tapped}$) if the difference between two consecutive readings was less than 2%. Compared to the USP method above, this method requires less material to perform.

2.2.2.4. Envelope and density analyzer (Geopyc®)

Powders with different bulk densities would experience different stresses during tapping. To minimize such variability, it was proposed to replace tapping with a controlled stress (Thalberg et al. 2004). This can be achieved using an envelope density analyzer (Geopyc®, model 1365, Micromeritics, Norcross, GA, USA). This method also requires less material than the two preceding tapped density-based methods. Here, a powder was slowly introduced into a 25.4 mm diameter graduated cylindrical glass cell to reach an initial bulk volume of approximately 13 mL and read to the nearest graduated unit. The filled cylinder was weighed to determine the weight of filled powder before being mounted horizontally on to the instrument. The cylinder was rotated while compressing the powder with a piston at 0.1 MPa (51 N) for 10 times (Fig. 2c). The displacement distance at the end of each compression was recorded, from which the density of the powder was calculated. The average of 10 measurements was reported. The compressed bulk

density was used to replace the tapped density (ρ_{tapped}) term in Eq. 4 and Eq. 5 to calculate HR and CI, respectively.

2.2.2.5. Minimum orifice diameter

Powder flowability can also be quantified by measuring the rate of a powder flowing through an orifice with a fixed diameter (USP, 2020a). However, this technique is only useful for free-flowing materials and a general scale for categorizing powder flowability is not available. For this reason, we used the minimum orifice diameter, which can be measured by Flodex[™] (Hanson Research Corp., Chatsworth, CA), to characterize a wide range of materials with different flowability. This method evaluates flowability by determining the minimum size of an orifice through which a powder can flow on its own weight. A powder was poured through a funnel into the loading cylinder to form a powder bed with a flat surface approximately 1 cm from the top of the cylinder (150 mL) (Zhou et al., 2020). The powder bed rests on a disk with an accurately known hole size. After the powder was allowed to settle for approximately 30 s to allow the possible flocculi formation, a lever was release to open the orifice. The flow behaviors of the powder were observed from the top and a positive result was noted when a hole was observed. This experiment was repeated using disks with different diameters (Gioia, 1980). The smallest hole diameter for the powder to flow through in all five attempts was taken as the minimum orifice diameter (*d*_{min}).

2.2.2.6. Shear cell

Shear cell method is established for flow characterization and hopper or bin design (USP, 2020a). During large-scale pharmaceutical production, a powder on the bottom of a hopper is consolidated more by the weight of the powder bed above it, the extent of which depends on the batch size, bulk density, and hopper design. Shear cell can measure shear strength of a powder under controlled normal stresses, from which yield locus and flow function can be determined (USP, 2020a). Several types of shear cell are available, such as translational (Jenike shear cell), annular cell (Schulze shear cell), and rotational cell (Peschel shear cell) (USP, 2020b). An annular shear cell tester (RST-XS; Dietmar Schulze, Wolfenbüttel, Germany) with a XS-Mr shear cell (30 mL cell volume) was used in this work. Data was collected using the 230 method (Shi et al., 2011) and all measurements were done in triplicate. Briefly, an aerated powder was filled in the shear cell with care to avoid compression on the powder. Then, powder was sheared at each of 1, 3, 6

kPa pre-shear normal stresses. After pre-shearing, the powder was sheared under 5 normal stresses between the lowest normal stress of 230 Pa and the corresponding pre-shear normal stress. A yield locus was constructed from the maximum shear stress at each normal stress, from which Mohr circles were drawn to determine the major principal stress (σ_1), and unconfined yield strength (σ_c).

A flowability index (ffc) was calculated using Eq. 6 (Schulze, 2021; Sun, 2016).

$$ff_c = \sigma_1 / \sigma_c$$
 Eq. 6

3. Results and discussion

243

246

247

248

249

250

251

252

- 3.1. Comparison within methods
- 245 3.1.1. Angle of repose (AoR)
 - AoR values from the fixed base and fixed height methods strongly correlate (R² = 0.939) (Fig. 3). However, based on the criteria in Table 1, slight differences led to different flow category levels for three out of the 21 powders, i.e., lactose monohydrate, NaCl, and CP-GRS (Table 3). In all three cases, the results from the fixed base method were always 1 level higher than that from the fixed height method. Thus, while the two methods yield globally similar assessment on flow for a range of materials, the fixed base method tends to predict better flow than the fixed height method. If decisions are made based on AoR data, the fixed height method produces more conservative predictions and, hence, wider safety zone for successful powder handling.

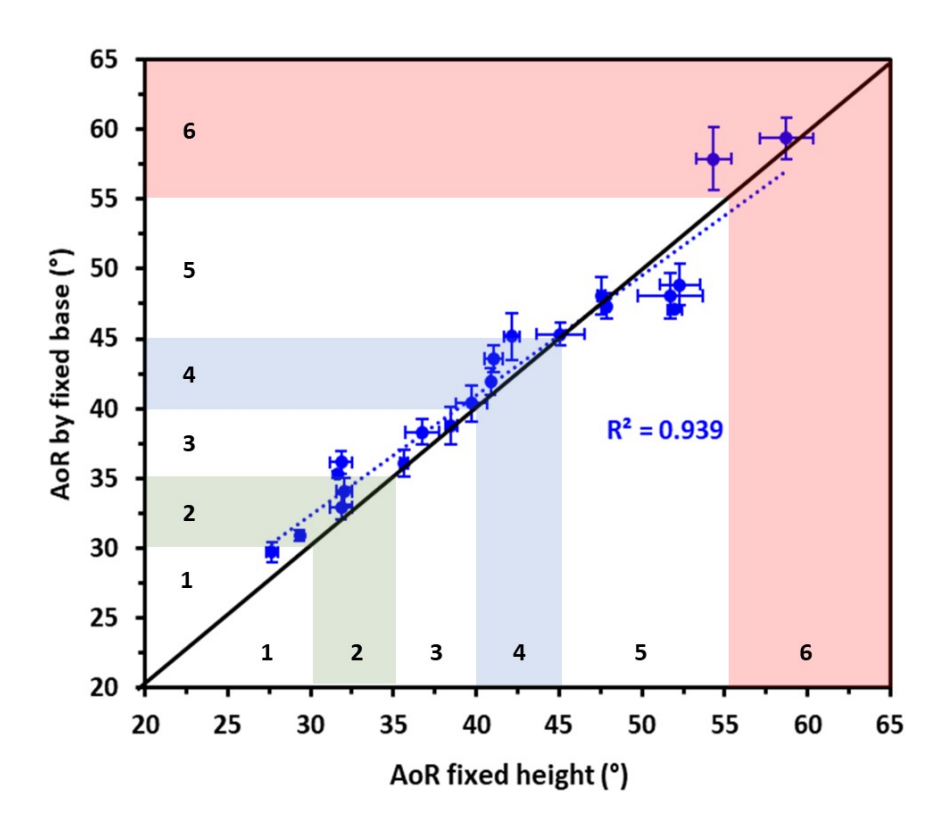


Fig. 3. Correlation between AoR measured using the fixed-height and fixed-base methods (n = 3). The solid line is the line of identity. The dashed line is the regression line of data points. Flow levels from 1-6 are indicated.

For materials in the "excellent (level 1)" to "passable (level 4)" flow categories, heap often collapsed (a phenomenon also known as "flooding") before the tip of the cone reached the funnel tip in the fixed height method. This result is in agreement with a previous study where free flowing materials were investigated (Train, 1958). For this reason, a larger amount of powder is required to perform the fixed height method for such materials.

During the AoR measurement, particles just exiting the funnel will pile up with a large base angle so that the resolved gravitational force parallel to the slope is higher than the interparticle friction and/or cohesion. Consequently, particles will roll down from the top to the base, which lowers the angle of the pile at the base. When the critical AoR is attained, particles falling from the funnel roll down the slope due to their initial momentum, which lowers the base angle. Subsequently, particles stop rolling in the lower portion of the pile due to the lower resolved gravitational force. New incoming particles from the funnel will gradually deposit from the base

to the top of the pile. This results in proportional enlargement of the base radius and pile height so that a constant AoR is maintained. Based on this mechanism, a more cohesive material forms a pile with a larger AoR. Consequently, a higher pile is formed for a more cohesive powder if the size of the base is fixed.

Table 3. AoR values and flow catgorization of 21 excipients studied in this work.

	Fixed heig	ght method	Fixed base method		
Excipients	Average (SD)	Flow category level	Average (SD)	Flow category level	
Avicel® PH101	47.6 (0.3)	5	48.1 (0.6)	5	
Avicel® PH102	39.7 (0.2)	3	40.3 (0.9)	3	
Avicel® PH105	58.7 (1.6)	6	59.4 (1.5)	6	
Comprecel® M101	52.0 (0.5)	5	47.1 (0.2)	5	
Comprecel® M102	42.1 (1.0)	4	45.2 (1.3)	4	
lactose monohydrate	54.3 (1.0)	5	57.9 (2.3)	6	
Fast-Flo®	31.6 (1.0)	2	35.3 (1.3)	2	
Flowlac®	36.7 (0.5)	3	38.3 (1.7)	3	
Supertab® 24AN	38.5 (0.1)	3	38.8 (0.3)	3	
nGRS	51.7 (1.9)	5	48.1 (1.7)	5	
sGRS	27.7 (0.3)	1	29.7 (0.7)	1	
Era-tab [®]	31.9 (0.7)	2	32.9 (0.9)	2	
Pearlitol® 160C	47.9 (0.3)	5	47.3 (1.4)	5	
NaCl	31.9 (0.6)	2	36.1 (0.8)	3	
Microcelac [®]	35.6 (0.2)	3	36.1 (0.9)	3	
Combilac [®]	32.0 (0.5)	2	34.1 (1.0)	2	
CP-GRS	29.3 (0.2)	1	30.9 (0.4)	2	
MCC PH101:102 (1:1)	41.0 (0.6)	4	43.6 (1.0)	4	
MCC PH101:102 (1:2)	40.9 (0.1)	4	41.9 (0.9)	4	
MCC PH101:102 (2:1)	45.1 (1.4)	4	45.3 (0.8)	4	
nGRS:MCC:LM (3:1:1)	52.3 (1.2)	5	48.9 (1.5)	5	

For cohesive powders, such as lactose monohydrate and Avicel® PH105, the piling process may not proceed smoothly. For example, adding a large quantity of powder into the funnel can lead to funnel obstruction. Moreover, AoR measurement of cohesive powders is complicated by collapsing of the pile under certain conditions, resulting in sections of the pile with different slopes (Fig. 4a). The angle of the base portion of the pile (α_s) is the smallest (i.e., better flow) because the powder contains more entrapped air when the collapsed powder moving down from the top of the

pile. The top section of the heap has the largest angle (α_m) since it does not have a history of collapsing. The middle section of the pile is a transition from the initial steep heap to the base zone, exhibiting an intermediated angle (α_i) (Fig. 4b) (Staniforth, 2001). For powders exhibiting such behaviors, α_i was used in this study. AoR of such powders may be measured also by using mixtures with a non-cohesive powder in various ratios and extrapolating AoR to pure cohesive powder based on observed relationship between AoR and mixture composition (Staniforth, 2001).

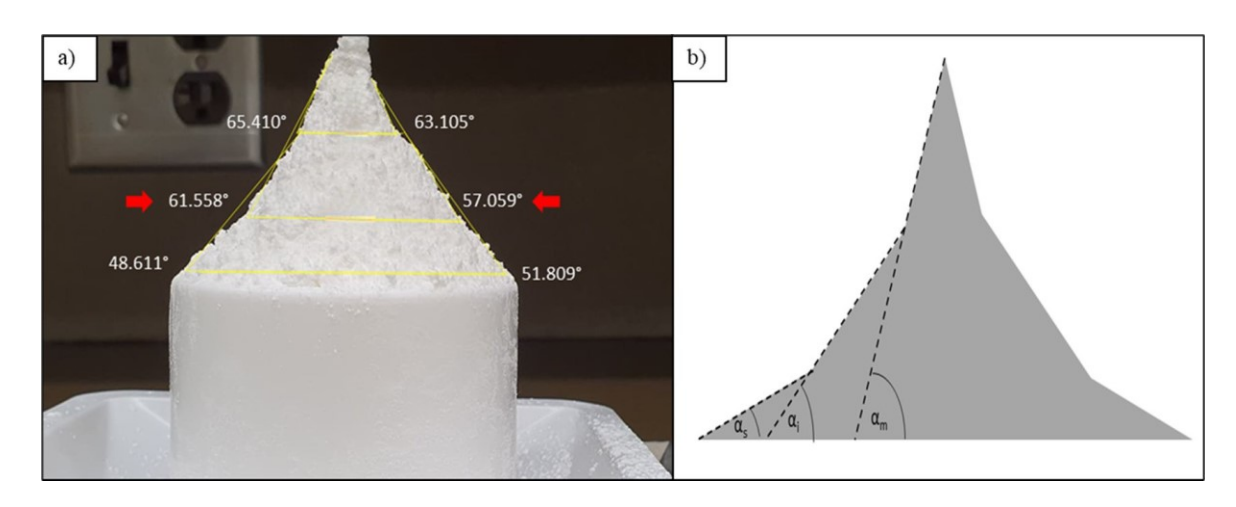


Fig. 4. Piling by a cohesive powder for AoR measurement a) fine lactose monohydrate in this study, b) an AoR model (modified from Staniforth, 2001)

3.1.2. Compressibility index and Hausner ratio

292

293

294

295

296

297

298

299

300

301

302

303

304

305

306

307

308

309

310

311

312

313

314

315

316

317

To collect volume or density data for calculating CI and HR, we used three techniques, a) tapped density tester, b) manual tapping, and c) Geopyc[®]. The tapped density tester method per the USP specifications (USP, 2020c) was used as a standard technique for comparison. Both the manual tapping and the Geopyc® methods generated CI and HR values strongly correlating with those from the USP tapped density method, but the manual tapping data is more strongly correlated based on the higher R² (Fig. 5). This data suggests that the manual tapping method is an acceptable alternative method to the USP tapped density method, when the latter cannot be performed. The tapped density tester data is also in good agreement with the Geopyc® data for good flow materials (small CI and HR), but the Geopyc® method tends to generate CI and HR values higher than that by the tapped density tester (Fig. 5), i.e., it tends to predicts poorer flowability for poorly flowing powders. This is similar to a previous observation where HR values based on the Geopyc[®] method were 5-10% higher than those from the tapped density tester for several cohesive powders (Thalberg et al., 2004). Such a difference is attributed to the high sensitivity of the bulk density of a bed of cohesive powder to an applied low compressive pressure. Because of the negligible friction, the whole powder in the Geopyc® cylinder was uniformly compressed by the applied external force (Thalberg et al., 2004). However, the pressure on the powder in a tapped cylinder increases with depth (Buanz, 2021; Staniforth, 2001). For cohesive powders, the low pressure (0.1 MPa) applied in the Geopyc® method was still higher than the average stress due to powder weight during the tapped density method. Hence, more consolidation of the powder bed was observed. Despite the different numerical CI and HR values, the flow classification was only minimally impacted (Table 4). Such degree of variations in flow categorization is comparable to that due to different cylinder size, tapping counts, and powder mass used in the test (USP, 2020a). Therefore, the USP tapped density method could be replaced with either material-sparing methods without major consequence with flow categorization.

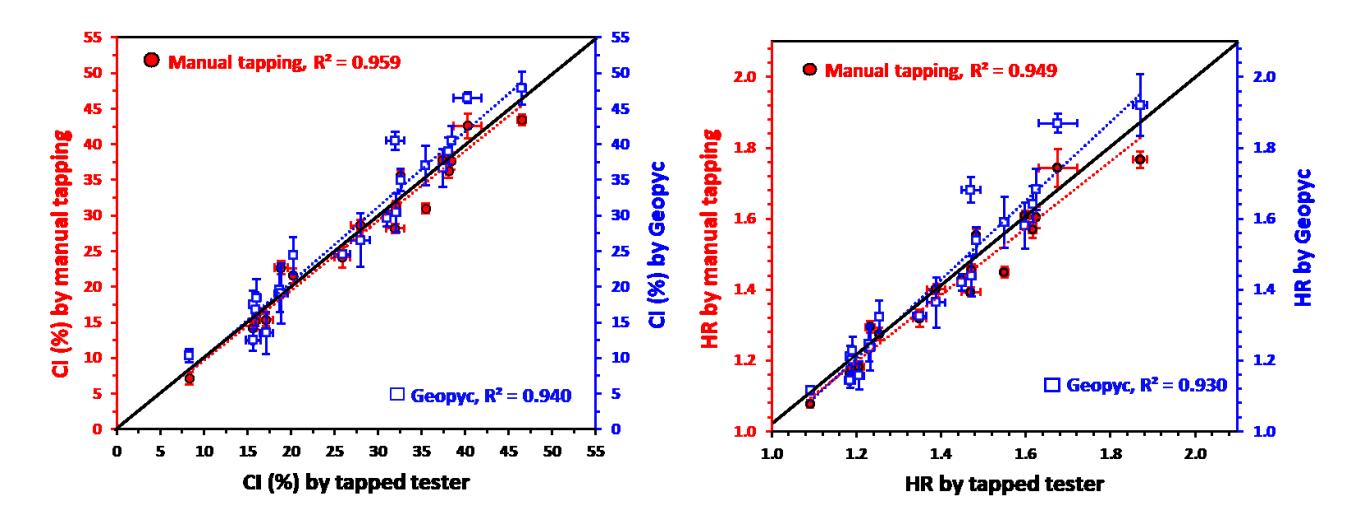


Fig. 5. Relationships among flow parameters calculated using data obtain by 3 different methods (tapped density tester, manual tapping, and Geopyc®). a) CI and b) HR. Solid lines are the lines of identity. Dashed lines are the regression lines of data points.

Table 4. Flow categorization of 21 sample powders based on CI and HR (n = 3).

	CI (%)					HR						
	Таррес	l tester	Manual	tapping	Geo	рус	Tapped	tester	Manual t	apping	Geo	
Compounds	Average (SD)	Flow category	Average (SD)	Flow category	Average (SD)	Flow category	Average (SD)	Flow category	Average (SD)	Flow category	Average (SD)	Flow category
Avicel® PH101	32.6 (0.3)	6	35.6 (0.8)	6	35.0 (1.6)	6	1.48 (0.01)	6	1.55 (0.02)	6	1.54 (0.04)	6
Avicel® PH102	25.9 (0.9)	5	24.1 (1.4)	4	24.6 (0.1)	4	1.35 (0.02)	5	1.32 (0.03)	4	1.33 (0.00)	4
Avicel® PH105	40.3 (1.6)	7	42.6 (1.8)	7	46.5 (0.7)	7	1.68 (0.04)	7	1.74 (0.05)	7	1.87 (0.03)	7
Comprecel® M101	38.1 (0.3)	7	36.2 (1)	6	39.0 (1.9)	7	1.62 (0.01)	7	1.57 (0.02)	6	1.64 (0.05)	7
Comprecel® M102	35.5 (0.4)	6	31 (0.7)	5	37.0 (2.8)	6	1.55 (0.01)	6	1.45 (0.02)	5	1.59 (0.07)	6
lactose monohydrate	46.5 (0.5)	7	43.4 (0.7)	7	47.9 (2.3)	7	1.87 (0.02)	7	1.77 (0.02)	7	1.92 (0.09)	7
Fast-Flo®	16.1 (0.5)	3	16.6 (0.2)	3	18.5 (2.6)	3	1.19 (0.01)	3	1.20 (0.00)	3	1.23 (0.04)	3
Flowlac®	18.8 (0.7)	3	22.7 (1)	4	19.0 (4.2)	3	1.23 (0.01)	3	1.29 (0.02)	4	1.24 (0.07)	3
Supertab® 24AN	20.3 (0.3)	3	21.6 (1.1)	4	24.4 (2.6)	4	1.25 (0.01)	3	1.28 (0.02)	4	1.32 (0.05)	4
nGRS	37.4 (0.4)	6	37.8 (0.6)	7	36.6 (2.7)	6	1.6 (0.01)	7	1.61 (0.02)	7	1.58 (0.07)	6
sGRS	17.1 (0.7)	3	15.4 (0.8)	2	13.5 (2.9)	2	1.21 (0.01)	3	1.18 (0.01)	2	1.16 (0.04)	2
Era-tab [®]	15.9 (0.3)	3	15.1 (1.1)	2	16.8 (2.3)	3	1.19 (0.00)	3	1.18 (0.02)	2	1.20 (0.03)	3
Pearlitol® 160C	32.0 (1.0)	6	28.2 (0.7)	5	40.5 (1.3)	7	1.47 (0.02)	6	1.39 (0.01)	5	1.68 (0.04)	7
NaCl	8.3 (0.1)	1	7.1 (0.8)	1	10.3 (0.9)	1	1.09 (0.00)	1	1.08 (0.01)	1	1.12 (0.01)	2
Microcelac®	18.7 (0.3)	3	18.9 (0.2)	3	19.6 (3.1)	3	1.23 (0.00)	3	1.23 (0.00)	3	1.25 (0.05)	3
Combilac®	15.7 (0.4)	3	14.2 (0.4)	2	17.5 (1.9)	3	1.19 (0.01)	3	1.17 (0.01)	2	1.21 (0.03)	3
CP-GRS	15.6 (0.8)	3	12.5 (0.3)	2	12.5 (1.5)	2	1.19 (0.01)	3	1.14 (0.00)	2	1.14 (0.02)	2
MCC PH101:102 (1:1)	31 (0.4)	5	29.9 (0.6)	5	29.6 (1.1)	5	1.45 (0.01)	5	1.43 (0.01)	5	1.42 (0.02)	5
MCC PH101:102 (1:2)	28 (1.1)	5	28.6 (0.7)	5	26.6 (3.7)	5	1.39 (0.02)	5	1.40 (0.01)	5	1.36 (0.07)	5
MCC PH101:102 (2:1)	32.1 (0.4)	6	31.3 (0.8)	5	30.4 (2.7)	5	1.47 (0.01)	6	1.46 (0.02)	6	1.44 (0.06)	5
nGRS:MCC:LM (3:1:1)	38.5 (0.2)	7	37.6 (1.2)	6	40.5 (2.0)	7	1.62 (0.00)	7	1.60 (0.03)	7	1.68 (0.06)	7

3.2. Comparison between methods

324

325

326

327

328

329

330

331

332

333

334

335

336

337

338

339

340

341

342

343

344

345

346

347

348

349

350

3.2.1. Correlation between AoR and CI/HR

Due to the strong correlation among the two methods of AoR measurement and the three methods for CI/HR measurements, only AoR by the fixed base and CI/HR values by tapped density tester were selected for comparing among methods in this work. In this set of powders, NaCl appears to be an outlier as a significantly lower CI is observed compared to powders with comparable AoR (Fig. 6). This is attributed to the high packing efficiency of NaCl, due to the cubic-like shape, smooth surface, and high density of NaCl crystals, which makes its powder bed more resistant to further densification by tapping (i.e., low compressibility). Therefore, NaCl was excluded from subsequent effort to correlate AoR with CI since it is not representative of typical pharmaceutical powders. This lead to a relatively strong positive correlation (Fig. 6, R² = 0.896).

For relatively free-flowing powders (AoR < 40°), CI value only varied within a narrow range. Thus, differences in particle density, friction, and other properties can exert significant influence on rolling of particles down the slope of a pile, i.e., AoR value, but not on CI values because those powders can all pack efficiently during initial powder filling and undergo comparable degree of densification during tapping. Therefore, correlation between AoR and CI is stronger for more cohesive powders (AoR > 40°), which means that a powder with a high AoR tends to exhibit a high CI. The observed strong correlation between AoR and CI in this work is in agreement with correlations between AoR and CI/HR observed in several earlier studies using metal powders (Geldart et al., 2006; Marchetti and Hulme-Smith, 2021), pharmaceutical powders (Goh et al., 2018; Tan and Newton, 1990; Tay et al., 2017; Thalberg et al., 2004), and spherical glass beads (Riley and Mann, 1972). We note that deviation of a fine ($D_{50} = 12.1 \mu m$) lactose powder from a linear relationship was observed in a previous study (Tay et al. 2017). The explanation for the deviation was that larger agglomerates formed by cohesive and fine lactose particles dictate flow behavior during AoR measurement, but the primary particles dictate behaviors during CI measurements, hence, the mismatch (Tay et al., 2017). This was not observed in this study.

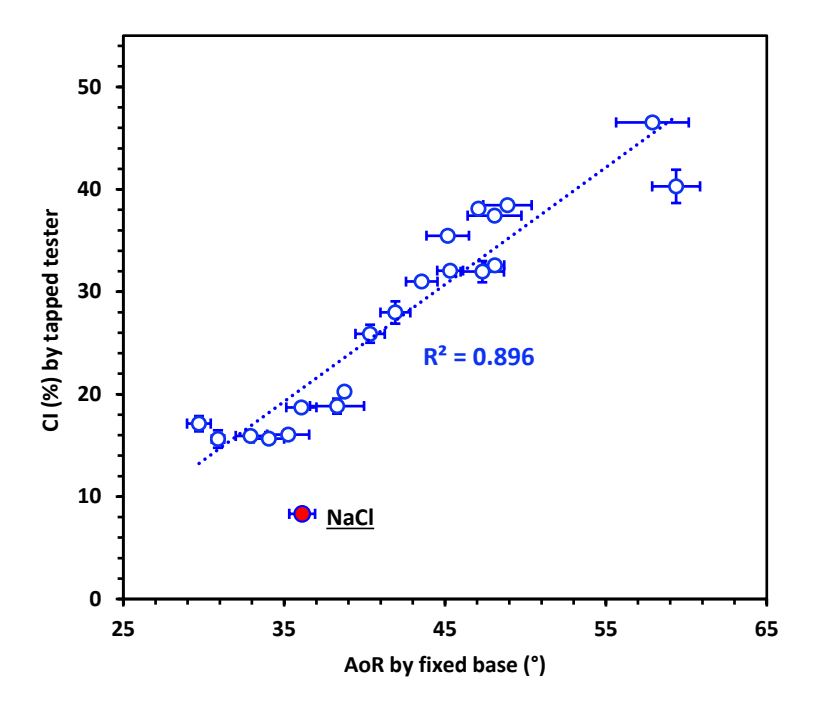


Fig. 6. The correlation between AoR by fixed base and CI by tapped density tester

3.2.2. Minimum orifice diameter (d_{min}) and its correlation with other flow parameters

A larger opening size is generally required for a more cohesive powder to initiate flow (i.e., break the arch) by gravitational force. It has also been observed that free-flow materials generally pass through a hole smoothly, but most cohesive materials tend to fall down at once when the opening size reaches d_{\min} . This phenomenon was explained as the weight of the cylindrical powder plug above the opening overcoming the side internal friction (Gioia, 1980), which leaves behind a cylinder-like tunnel (Fig. 7a). In contrast, a free-flowing powder passes through the opening smoothly to form an inverted cone-like cavity inside the sample loading chamber at the end of the experiment (Fig. 7b). In this study, a cylindrical cavity was likely observed for powders that require $d_{\min} \ge 18$ mm (Table 5). It is interesting to note that, the three grades of microcrystalline cellulose (MCC), Avicel® PH102, Comprecel® M101 and M102, all have $d_{\min} = 18$ mm, but both types of cavity patterns were observed. The Avicel® PH102 and Comprecel® M102 consist of larger particles that passed through the disc hole gradually to form an inverted cone-like cavity. In contrast, the finer Comprecel® M101 powder formed a cylindrical cavity. Since flowability of the three powders follows the descending order of Avicel® PH102 > Comprecel® M102 > Comprecel®

M101 based on AoR and CI data (Tables 3 and 4), this observation suggests that both d_{\min} and cavity pattern should be considered for the flow evaluation by this technique. For powders requiring the same d_{\min} , the ones that form an inverted cone like funnel exhibit better flow properties.

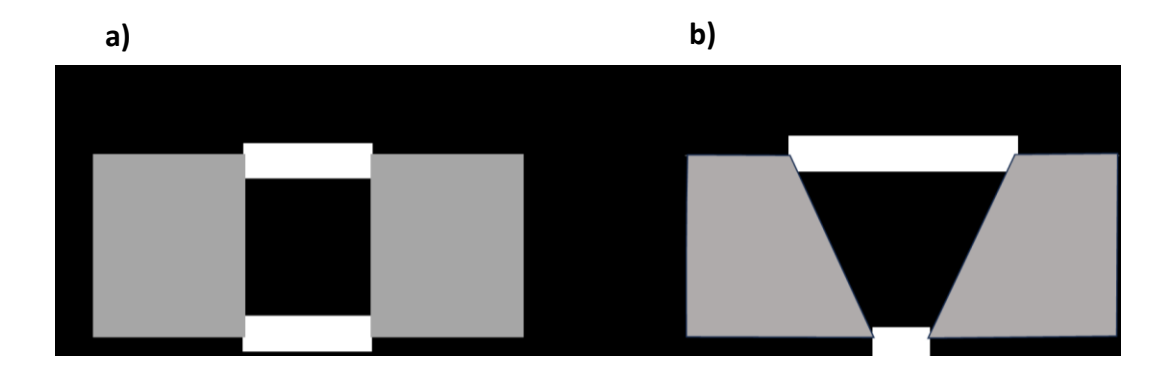


Fig. 7. Two patterns of the funnel cavity after flowing out the powder from the FlodexTM sample cell, a) cylindrical, b) inverted cone.

Table 5. Minimum orifice diameters (d_{min}) and flow patterns of 21 powders studied using FlodexTM

Excipients	Minimum orifice diameter (d_{min})	Flow pattern
Avicel® PH101	22	Cylindrical
Avicel® PH102	18	Inverted cone
Avicel® PH105	22	Cylindrical
Comprecel® M101	18	Cylindrical
Comprecel® M102	18	Inverted cone
lactose monohydrate	34	Cylindrical
Fast-Flo®	<4	Inverted cone
Flowlac®	5	Inverted cone
Supertab® 24AN	9	Inverted cone
nGRS	24	Cylindrical
sGRS	5	Inverted cone
Era-tab®	5	Inverted cone
Pearlitol® 160C	30	Cylindrical
NaCl	6	Inverted cone
Microcelac®	10	Inverted cone

Combilac®	<4	Inverted cone
CP-GRS	<4	Inverted cone
Avicel® PH101:102 (1:1)	20	Cylindrical
Avicel® PH101:102 (1:2)	20	Cylindrical
Avicel® PH101:102 (2:1)	22	Cylindrical
nGRS:MCC:LM (3:1:1)	22	Cylindrical

Both AoR and d_{\min} assess powder flowability based on the interplay between gravitational force and interparticulate friction or cohesion. Therefore, they are expected to correlate. In fact, a medium linear correlation was obtained for the set of powders in this study ($R^2 = 0.778$, Fig. 8). Due to a strong correlation between AoR and HR, some degree of correlation between d_{\min} and HR is also expected, which is also observed in this study ($R^2 = 0.798$, Fig. 8). These results are in agreement with a previous study, where AoR and d_{\min} ("Flowability index; FI") of aluminum and modified aluminum powders followed a similar trend (Jallo et al., 2010).

The FlodexTM measurement is intuitive and simple to perform. However, the opening size range of 4 mm – 34 mm means that it is not suitable for distinguishing either free-flowing powders ($d_{\min} < 4$ mm) or highly cohesive powders ($d_{\min} > 34$ mm). Therefore, for powders exhibiting extreme flowability (both very poor or very good), AoR and HR measurements hold advantage over measuring d_{\min} by FlodexTM.

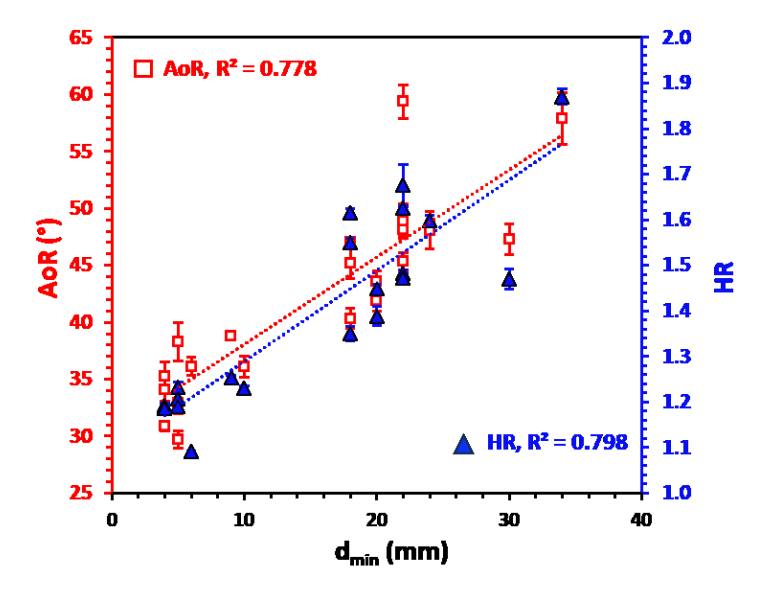


Fig. 8. Correlation of d_{\min} with AoR and HR

Table 6. f_c and f_c by shear cell of excipients measured at pre-shear stresses of 1, 3, 6 kPa (n = 3)

	Shear cell							
Evaluionto		fc (Pa)		ffc				
Excipients	1 kPa	3 kPa	6 kPa	1 kPa	3 kPa	6 kPa		
	Average (SD)	Average (SD)	Average (SD)	Average (SD)	Average (SD)	Average (SD)		
Avicel® PH101	685.33 (18.50)	1401.00 (84.43)	2452.33 (76.89)	3.37 (0.07)	4.85 (0.22)	5.63 (0.21)		
Avice ^{l®} PH102	335.33 (18.15)	647.33 (26.69)	998.00 (37.99)	6.03 (0.31)	9.30 (0.29)	12.08 (0.42)		
Avicel® PH105	1070.33 (37.98)	2336.33 (54.88)	3863.67 (43.00)	2.21 (0.03)	2.87 (0.06)	3.35 (0.04)		
Comprecel® M101	610.33 (18.58)	1217.67 (33.95)	1930.00 (106.08)	3.77 (0.09)	5.49 (0.11)	6.86 (0.36)		
Comprecel® M102	521.00 (6.00)	1011.67 (15.82)	1685.00 (54.81)	4.10 (0.09)	6.23 (0.06)	7.38 (0.20)		
lactose monohydrate	1077.67 (74.14)	1864.00 (47.79)	2865.33 (9.07)	1.99 (0.08)	3.26 (0.06)	4.13 (0.01)		
Fast-Flo®	207.00 (5.29)	284.00 (8.19)	295.67 (11.85)	8.70 (0.21)	18.48 (0.55)	35.25 (1.36)		
Flowlac®100	279.67 (12.06)	380.67 (7.02)	465.33 (10.41)	6.05 (0.27)	12.8 (0.32)	21.00 (0.38)		
Supertab® 24AN	202.33 (10.07)	284.67 (18.15)	379.00 (23.52)	9.55 (0.46)	20.15 (1.12)	30.00 (1.56)		
nGRS	519.00 (14.11)	979.67 (23.69)	1445.67 (105.63)	3.42 (0.06)	5.35 (0.12)	7.26 (0.59)		
sGRS	166.00 (1.00)	286.67 (11.72)	326.00 (21.00)	10.04 (0.07)	17.11 (0.69)	30.04 (1.81)		
Era-tab [®]	209.67 (3.21)	376.00 (17.52)	590.00 (41.87)	7.65 (0.17)	12.58 (0.47)	16.02 (1.04)		
Pearlitol® 160C	659.33 (13.58)	1074.00 (23.64)	1480.00 (87.54)	3.30 (0.06)	5.77 (0.05)	8.10 (0.39)		
NaCl*								
Microcelac®100	194.67 (14.43)	287.00 (12.49)	418.33 (17.21)	9.33 (0.70)	18.42 (0.70)	25.19 (1.24)		
Combilac [®]	158.67 (2.08)	277.00 (10.54))	410.67 (22.05)	11.06 (0.25)	18.44 (0.87)	24.72 (1.57)		
CP-GRS	175.67 (17.04)	274.33 (9.07)	357.00 (8.66)	9.62 (0.82)	18.12 (0.55)	27.49 (0.95)		
MCC PH101:102 (1:1)	472.00 (22.52)	920.33 (15.82)	1511.00 (50.48)	4.69 (0.26)	7.07 (0.10)	8.71 (0.33)		
MCC PH101:102 (1:2)	406.00 (26.85)	848.33 (40.67)	1444.00 (144.36)	5.23 (0.26)	7.59 (0.32)	9.11 (0.88)		
MCC PH101:102 (2:1)	471.33 (30.01)	987.00 (57.66))	1540.33 (61.5)	4.68 (0.20)	6.66 (0.33)	8.49 (0.38)		
nGRS:MCC:LM (3:1:1)	550.33 (61.17)	1139.00 (26.51)	1684.00 (38.57)	3.41 (0.42)	4.90 (0.09)	6.51 (0.12)		

^{*}Reliable shear cell data of NaCl could not be collected due to severe slip-stick phenomenon during the test.

3.2.3. Shear cell parameters and its correlation with other flow parameters

3.2.3.1. Shear cell parameters for flowability assessment

Since a higher unconfined yield strength, σ_c , means stronger particle-particle interaction, a higher shear stress is required to initiate powder flow for a powder with a higher σ_c (Schulze, 2021). Thus, a powder with a higher σ_c under the same normal stress exhibits poorer flowability. In contrast, the flowability index (ff_c) considers both σ_c and external stress (Eq. 6), where a larger ff_c corresponds to better flowability. This is observed by all powders in this study (Table 6). Similarly, a higher shear stress is required to initiate flow of a more consolidated powder under a higher normal stress because of stronger interactions between particles in a more consolidated powder bed (Hou and Sun, 2008; Schulze, 2021). This is also observed in this work (Table 6).

3.2.3.2. Correlation of ffc with AoR and CI

The correlation between AoR and ff_c under 1, 3, and 6 kPa for all 21 samples is moderate (Fig. 9), with R² equals to 0.831, 0.754, and 0.670, respectively. Some previous studies reported correlation of shear cell parameters with AoR and/or CI/HR for pharmaceutical capsule fillers (Tan and Newton, 1990), different grades of MCC (Hou and Sun, 2008), metal powders (Marchetti and Hulme-Smith, 2021), and metformin formulations (Goh et al., 2018). During shear cell testing, the gravitational force is negligible compared to the normal stress applied. Among 3 different preshear forces, the 1 kPa data correlates more strongly with AoR and CI data, likely because it is closest to the "zero" applied external stress during AoR and CI data collection.

Correlation between ff_c at all pre-shear stresses and AoR and CI is poorer for more free-flowing powders (highlighted in the dotted box in Fig. 9a and 9b). Avicel PH102 was previously established as a powder lying at the boundary between the acceptable and unacceptable flowability regions for high speed tableting (Sun, 2010). It is interesting to note that Avicel PH102 (AoR \approx 40, CI \approx 25%) is near the borderline between the "Fair-Aid not needed (AoR 36-40)" and "Passable-May hang up (AoR 41-45)" flow classes by the measure of AoR, as well as the borderline between "Passable (21-25%)" and "Poor (26-31%)" flow classes by the measure of CI. This agreement suggests the AoR and CI based powder flowability categorization is valid. For free-flowing powders, ff_c values are usually large and scattered. Thus, shear cell test is more suitable for accurately quantifying flowability of poorly flowing powders. For materials with

flowability worse than Avicel PH®102, stronger correlation of ff_c with AoR and CI is observed (Fig. 9c and 9d). Therefore, ff_c , AoR, and CI are comparable in rank ordering flowability of poorly flowing powders, while AoR and CI appear to be more reliable for rank-ordering free-flowing powders.

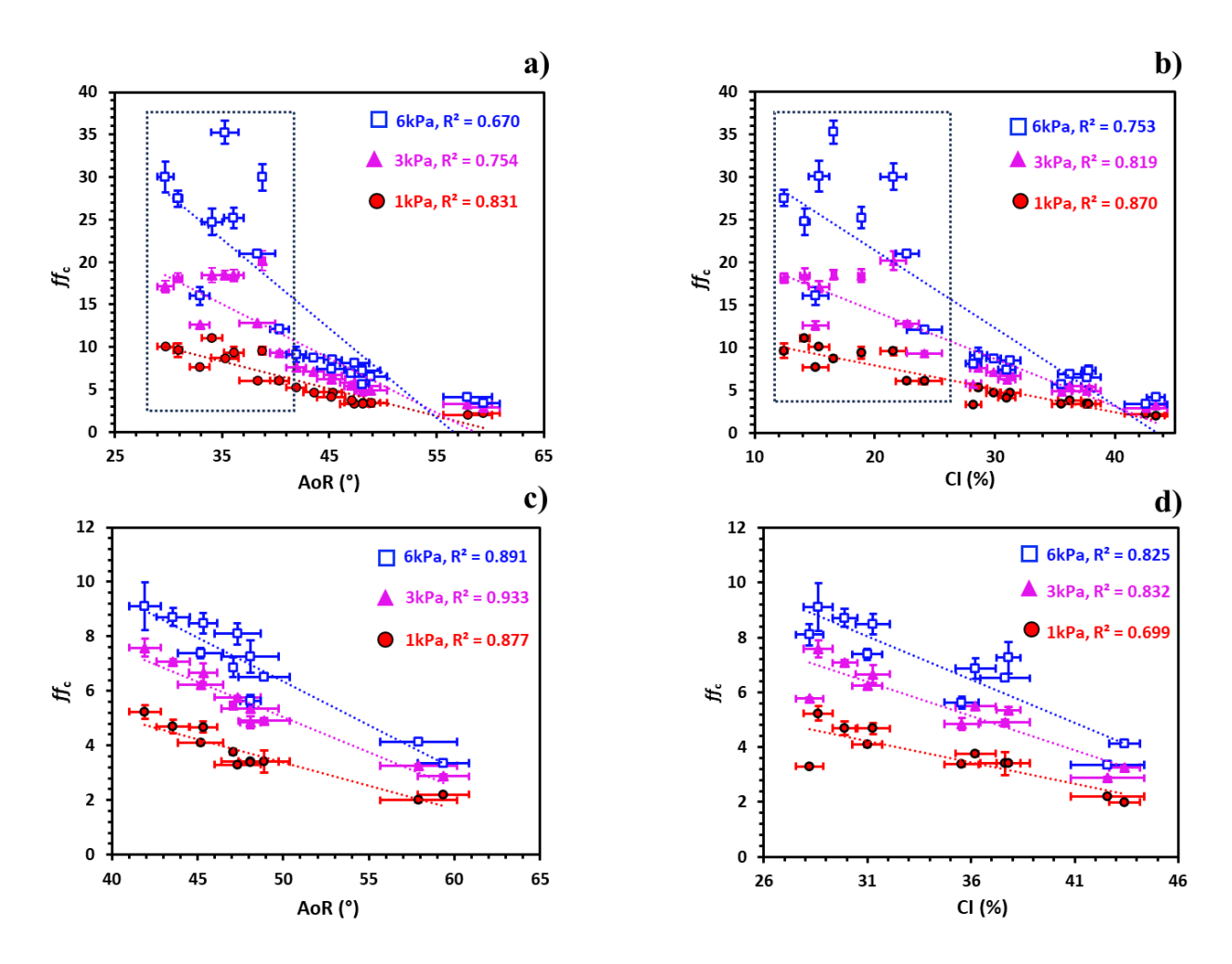


Fig. 9. The correlation between shear cell flow parameter f_c at 1, 3, 6 kPa normal stresses and **a)** AoR (all 21 powders), **b)** CI (all 21 powders), **c)** AoR (only powders with poorer flowability than Avicel PH102), **d)** CI (only powders with poorer flowability than Avicel PH102)

3.2.3.3. Correlation between ff_c and d_{min}

The correlation between d_{min} and f_c (at 1, 3, 6 kPa pre-shear stresses) is moderate, with R² equals to 0.784, 0.769, and 0.743, respectively. The stronger correlation at a lower normal stress

level is consistent with the reported stronger correlation between f_c derived from FlodexTM and f_c extrapolated from shear cell under the low stress condition (in the order of 100 Pa) (Zhou et al., 2020). The global correlation is weakened, in part, because of the inability of FlodexTM to distinguish free-flowing materials with $d_{min} < 4$ mm (see data points highlighted in the dot oval in Fig. 10). This limitation was also reported in an earlier study (Zettler et al., 2016). However, accurately rank-ordering free-flowing materials has little practical value as flow related problems normally are caused by poor flowability.

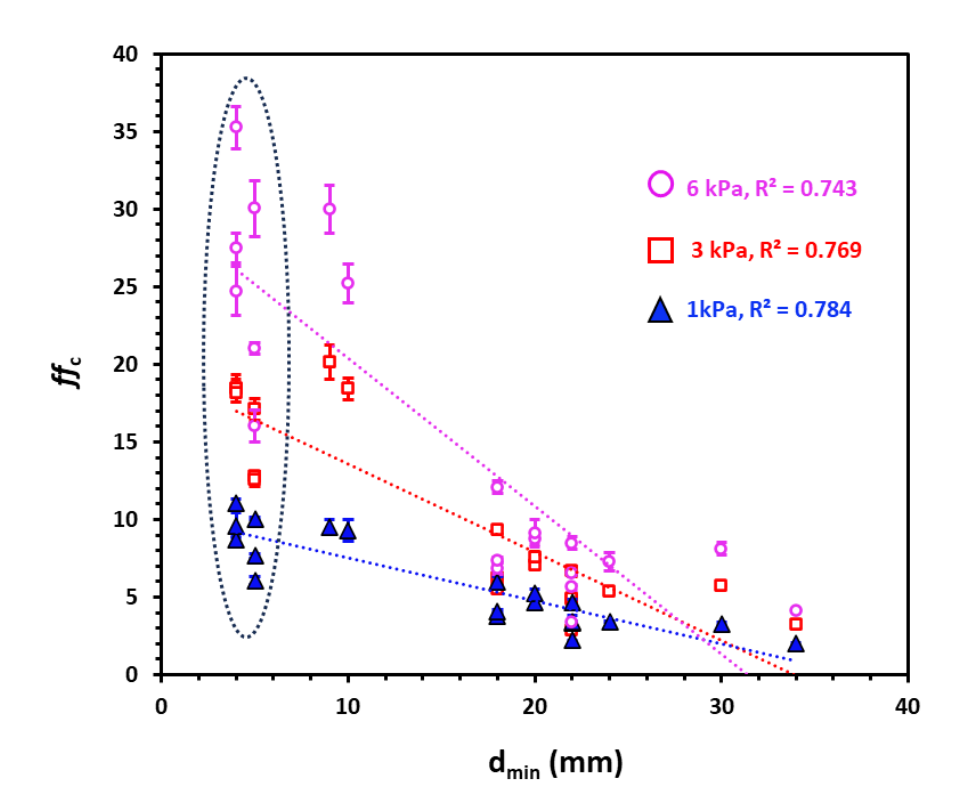


Fig. 10. The correlation between d_{\min} and f_{c} at pre-shear stresses of 1, 3, 6 kPa.

3.3. Overall comparison

AoR values from the fixed base AoR and fixed height AoR methods strongly correlate. Therefore, the two techniques are practically interchangeable. CI and HR values from all three techniques (tapped density tester, manual tapping, and Geopyc®) also strongly correlate, but the Geopyc® method produces higher values for cohesive materials than the other two techniques. The manual tapping method holds an advantage over the Geopyc® because it does not require a special

instrument and its data correlates strongly with that of the USP method. A comparison of the four methods for powder flow characterization, along with typical powder amounts required for each test, is given in Table 7, based on sensitivity in distinguishing flow property of powders, ease of use, and accessibility.

Table 7. Comparison of ability to distinguish powder flow properties by different flow test methods.

	Flow b	ehavior	Powder amount	
Flow test	Poor flow	Good flow	required for tests c	
AoR^a	good	good	5-20 g	
CI/HR	good	good	Tapped tester 20-30 g Manual tapping 10 g Geopyc 4-7 g	
Minimum orifice diameter ^b	good	poor	30-60 g	
Shear cell	excellent	medium	10-20 g	

Shear cell excellent medium 10-20 g

a: May encounter complicated measurement and sample handling problems for very cohesive powders

In general, strong correlation was observed among different measurements in poor flow region. However, caution should be exercised when choosing a technique for assessing powder flowability. The shear cell and CI/HR method are more suitable for poorly flowing powders than AoR and Flodex[™] measurements. However, shear cell test is less sensitive than AoR and CI/HR in distinguishing materials that exhibit good flow behaviors. The slip-stick phenomenon observed when testing free flowing powders, such as NaCl, further limits the application of shear cell test. The ability of Flodex[™] to quantify free-flowing powders is limited by the minimum 4 mm opening, as smaller opening diameters may face the issue of particle jamming. The AoR measurement is less suitable for poorly flowing powders due to the complicated measurement (such as multiple angles) and sample handling problem (such as a funnel obstruction). Knowledge obtained in this research facilitates the selection of a suitable flow method for powders. However, we recommend employing multiple techniques, when possible, to more holistically characterize the flowability of

^{b.} Applicability for powders exhibiting extreme flow behaviors (either very poor or very good) is limited

^c NaCl is excluded from the ranges given in the table.

powders. The selection of flow testing methods should also consider the amount of material required for testing, especially in the early stage of novel drug products development, and the availability of test equipment (Howard , 2007). Given the minimum requirement on equipment, we recommend to always collect CI/HR values as baseline powder flow characterization. For the purpose of rank-ordering powders, shear cell method likely perform well for poorly flowing cohesive powders while the AoR is more appropriate for free-flowing powders. Regardless of the method employed, it is beneficial to include Avicel PH102 in the list of tested powders to facilitate categorization, by the way of comparison, of flow behaviors of a powder of interest.

4. Conclusion

We have systematically evaluated the powder flow methods in USP <1174>, such as AoR by fixed base, CI/HR by tapped density tester, and shear cell, as well as their modified versions, i.e., AoR by fixed height, CI/HR by manual tapping and Geopyc[®], flow through an orifice (d_{min} from FlodexTM), using 21 powders. While these measurements are generally correlated, each of them has unique advantages and limitations. It is therefore advisable to apply all these techniques, if possible, to fully profile flow properties of powders. The validity of the classification of powder based on AoR and CI values is supported by the observation that Avicel[®] PH102 falls near the boundary between acceptable and non-acceptable classes by both measures.

Acknowledgements

W.T. was supported by the Royal Golden Jubilee (RGJ) Ph.D. Program (Grant. No. PHD/0160/2561), through the Thailand Research Fund (TRF), the National Research Council of Thailand (NRCT), the Thailand Science Research and Innovation (TSRI), and Khon Kaen University grant. C.C.S thanks the National Science Foundation for support through the Industry University Collaborative Research Center grant IIP-2137264, Center for Integrated Materials Science and Engineering for Pharmaceutical Products (CIMSEPP).

References

- Beakawi Al-Hashemi, H. M., & Baghabra Al-Amoudi, O. S. (2018). A review on the angle of repose of granular materials. *Powder Technology*, *330*, 397–417. https://doi.org/10.1016/j.powtec.2018.02.003
- Bharadwaj, R., Ketterhagen, W. R., & Hancock, B. C. (2010). Discrete element simulation study of a Freeman powder rheometer. *Chemical Engineering Science*, 65(21), 5747–5756. https://doi.org/10.1016/j.ces.2010.04.002
- Buanz, A. (2021). Powder characterization. In *Remington* (pp. 295–305). Elsevier. https://doi.org/10.1016/B978-0-12-820007-0.00016-7
- Chattoraj, S., Shi, L., & Sun, C. C. (2011). Profoundly improving flow properties of a cohesive cellulose powder by surface coating with nano-silica through comilling. *Journal of Pharmaceutical Sciences*, *100*(11), 4943–4952. https://doi.org/10.1002/jps.22677
- Freeman, R. (2007). Measuring the flow properties of consolidated, conditioned and aerated powders—A comparative study using a powder rheometer and a rotational shear cell.

 *Powder Technology, 174(1), 25–33. https://doi.org/10.1016/j.powtec.2006.10.016
- Gaisford, S., & Saunders, M. (2012). *Essentials of Pharmaceutical Preformulation* (1st ed.). Wiley. https://doi.org/10.1002/9781118423226
- Geldart, D., Abdullah, E. C., Hassanpour, A., Nwoke, L. C., & Wouters, I. (2006).

 Characterization of powder flowability using measurement of angle of repose. *China Particuology*, 4(3–4), 104–107. https://doi.org/10.1016/S1672-2515(07)60247-4
- Gioia, A. (1980). Intrinsic flowability: A new technology for powder-flowability classification.

 *Pharmaceutical Technology.

- Goh, H. P., Heng, P. W. S., & Liew, C. V. (2018). Comparative evaluation of powder flow parameters with reference to particle size and shape. *International Journal of Pharmaceutics*, *547*(1–2), 133–141. https://doi.org/10.1016/j.ijpharm.2018.05.059
- Hancock, B. C., Vukovinsky, K. E., Brolley, B., Grimsey, I., Hedden, D., Olsofsky, A., & Doherty, R. A. (2004). Development of a robust procedure for assessing powder flow using a commercial avalanche testing instrument. *Journal of Pharmaceutical and Biomedical Analysis*, 35(5), 979–990. https://doi.org/10.1016/j.jpba.2004.02.035
- Harnby, N. H., & Vandame, D. (1987). The use of bulk density determination as a mean of typifying the flow characteristics of loosely compacted powders under conditions of variable relative humidity. *Chemical Engineering Science*, 42(4), 879–888.
 https://doi.org/10.1016/0009-2509(87)80046-5
- Hassanpour, A., Hare, C., & Pasha, M. (Eds.). (2019). Powder Flow: Theory, Characterisation and Application. The Royal Society of Chemistry.https://doi.org/10.1039/9781788016100
- Hou, H., & Sun, C. C. (2008). Quantifying Effects of Particulate Properties on Powder Flow

 Properties Using a Ring Shear Tester. *Journal of Pharmaceutical Sciences*, 97(9), 4030–
 4039. https://doi.org/10.1002/jps.21288
- Howard A, S. (2007). Solids: Flow properties. In *Encyclopedia of Pharmaceutical technology* (3rd ed., Vol. 1, p. 3275). Informa Healthcare USA, Inc.
- Jallo, L. J., Schoenitz, M., Dreizin, E. L., Dave, R. N., & Johnson, C. E. (2010). The effect of surface modification of aluminum powder on its flowability, combustion and reactivity. *Powder Technology*, 204(1), 63–70. https://doi.org/10.1016/j.powtec.2010.07.017

- Kalman, H. (2021). Quantification of mechanisms governing the angle of repose, angle of tilting, and Hausner ratio to estimate the flowability of particulate materials. *Powder Technology*, 382, 573–593. https://doi.org/10.1016/j.powtec.2021.01.012
- Krantz, M., Zhang, H., & Zhu, J. (2009). Characterization of powder flow: Static and dynamic testing. *Powder Technology*, 194(3), 239–245.
 https://doi.org/10.1016/j.powtec.2009.05.001
- Lavoie, F., Cartilier, L., & Thibert, R. (2002). New Methods Characterizing Avalanche Behavior to Determine Powder Flow. *Pharmaceutical Research*, 19(6).
- Leturia, M., Benali, M., Lagarde, S., Ronga, I., & Saleh, K. (2014). Characterization of flow properties of cohesive powders: A comparative study of traditional and new testing methods. *Powder Technology*, 253, 406–423. https://doi.org/10.1016/j.powtec.2013.11.045
- Lüddecke, A., Pannitz, O., Zetzener, H., Sehrt, J. T., & Kwade, A. (2021). Powder properties and flowability measurements of tailored nanocomposites for powder bed fusion applications.

 *Materials & Design, 202, 109536. https://doi.org/10.1016/j.matdes.2021.109536
- Marchetti, L., & Hulme-Smith, C. (2021). Flowability of steel and tool steel powders: A comparison between testing methods. *Powder Technology*, *384*, 402–413. https://doi.org/10.1016/j.powtec.2021.01.074
- Montanari, D., Agostini, A., Bonini, M., Corti, G., & Ventisette, C. (2017). The Use of Empirical Methods for Testing Granular Materials in Analogue Modelling. *Materials*, 10(6), 635. https://doi.org/10.3390/ma10060635

- Müller, D., Fimbinger, E., & Brand, C. (2021). Algorithm for the determination of the angle of repose in bulk material analysis. *Powder Technology*, 383, 598–605.
 https://doi.org/10.1016/j.powtec.2021.01.010
- Rasband, W. (1997). *ImageJ* (1.53k) [Computer software]. National Institutes of Health. http://imagej.nih.gov/ij
- Riley, G. S., & Mann, G. R. (1972). Effects of particle shape on angles of repose and bulk densities of a granular solid. *Materials Research Bulletin*, 7(2), 163–169. https://doi.org/10.1016/0025-5408(72)90273-5
- Schulze, D. (2021). *Powders and Bulk Solids: Behavior, Characterization, Storage and Flow* (2nd ed.). Springer International Publishing. https://doi.org/10.1007/978-3-030-76720-4
- Shi, L., Feng, Y., & Sun, C. C. (2011). Origin of profound changes in powder properties during wetting and nucleation stages of high-shear wet granulation of microcrystalline cellulose.

 *Powder Technology, 208(3), 663–668. https://doi.org/10.1016/j.powtec.2011.01.006
- Staniforth, J. (2001). Powder flow. In *Pharmaceutics The Science of Dosage For Design* (2nd ed., Vol. 1, pp. 197–210). Churchill Livingstone.
- Sun, C. C. (2010). Setting the bar for powder flow properties in successful high speed tableting.

 *Powder Technology, 201(1), 106–108. https://doi.org/10.1016/j.powtec.2010.03.011
- Sun, C. C. (2016). Quantifying effects of moisture content on flow properties of microcrystalline cellulose using a ring shear tester. *Powder Technology*, 289, 104–108. https://doi.org/10.1016/j.powtec.2015.11.044
- Tan, S. B., & Newton, J. M. (1990). Powder flowability as an indication of capsule filling performance. *International Journal of Pharmaceutics*, 61(1–2), 145–155. https://doi.org/10.1016/0378-5173(90)90053-7

- Tay, J. Y. S., Liew, C. V., & Heng, P. W. S. (2017). Powder Flow Testing: Judicious Choice of Test Methods. AAPS PharmSciTech, 18(5), 1843–1854. https://doi.org/10.1208/s12249-016-0655-3
- Taylor, K., & Aulton, M. E. (2021). *Aulton's Pharmaceutics E-Book: The Design and Manufacture of Medicines*. Elsevier Health Sciences.
- Taylor, M. K., Ginsburg, J., Hickey, A. J., & Gheyas, F. (2000). Composite method to quantify powder flow as a screening method in early tablet or capsule formulation development.

 AAPS PharmSciTech, 1(3), 20–30. https://doi.org/10.1208/pt010318
- Thalberg, K., Lindholm, D., & Axelsson, A. (2004). Comparison of different flowability tests for powders for inhalation. *Powder Technology*, 146(3), 206–213.
 https://doi.org/10.1016/j.powtec.2004.08.003
- Train, D. (1958). Some Aspects of the Property of Angle of Repose of Powders. *Journal of Pharmacy and Pharmacology*, 10, 127–135. https://doi.org/10.1111/j.2042-7158.1958.tb10391.x
- USP. (2020a). <616> bulk density and tapped density of powders. In *The United States Pharmacopeia 43 and National Formulary 38* (Vol. 4, p. 6850).
- USP. (2020b). <1063> Shear cell methodology for powder flow testing. In *The United States Pharmacopeia 43 and National Formulary 38* (Vol. 5, p. 7567).
- USP. (2020c). <1174> Powder flow. In *The United States Pharmacopeia 43 and National Formulary 38* (Vol. 5, p. 7993).
- Zafar, U., Hare, C., Calvert, G., Ghadiri, M., Girimonte, R., Formisani, B., Quintanilla, M. A. S.,
 & Valverde, J. M. (2015). Comparison of cohesive powder flowability measured by
 Schulze Shear Cell, Raining Bed Method, Sevilla Powder Tester and new Ball

- Indentation Method. *Powder Technology*, *286*, 807–816. https://doi.org/10.1016/j.powtec.2015.09.010
- Zettler, A., Hilden, J., Koenig, M., Breslin, C., Aburub, A., Allgeier, M., Patel, P., & Mitra, B.
 (2016). Evaluation of Small-Scale Powder Flow Characterization Tests in the Prediction of Large-Scale Process Failures. *Journal of Pharmaceutical Innovation*, 11(3), 189–199. https://doi.org/10.1007/s12247-016-9258-5
- Zhou, X., Nauka, E., Narang, A., & Mao, C. (2020). Flow Function of Pharmaceutical Powders at Low-Stress Conditions Can Be Inferred Using a Simple Flow-Through-Orifice Device.

 Journal of Pharmaceutical Sciences, 109(6), 2009–2017.

 https://doi.org/10.1016/j.xphs.2020.02.017